ACS Energy LETTERS

Cite This: ACS Energy Lett. 2018, 3, 1887−1891

VIEWPOINT

Can SHG Measurements Determine the Polarity of Hybrid Lead Halide Perovskites?

Lead halide perovskites have excited a very large community of scientists and technologists. While there is understandable excitement at the possibility of commercialization of photovoltaic products in view of its extraordinary light-to-electricity conversion efficiency and easy processability using solution phases,[1−4] there is also widespread curiosity to understand the origin of such spectacular properties. Through extensive investigations, it is now well-established that these materials have the most unusual convergence of almost all properties that help achieve a high photovoltaic efficiency, namely, the right optical bandgap,[5,6] a high optical absorption coefficient,[7−9] slow electron−hole recombination,[10,11] long carrier diffusion lengths,[7,8,12] moderate excitonic binding energy,[13−15] high open-circuit voltage,[16] and indifference to the extent of defects[17] present, among others. Instead of satisfying the quest for understanding, such a wonderful confluence of desirable properties appears to have only enhanced the search for any underlying principle that may rationalize and unify many of these apparently distinct properties. One such possibility that has attracted the maximum attention, both for and against, is the question whether these materials are ferroelectric. Figure 1 illustrates the mechanism and advantages of a ferroelectric photovoltaic cell over a nonferroelectric one.

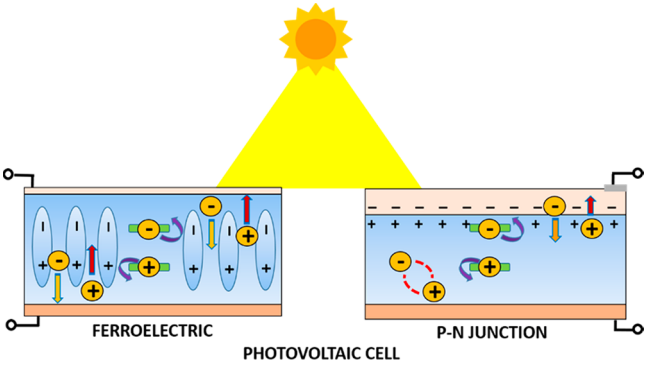

Figure 1. Schematic illustration of the processes and advantages of a ferroelectric photovoltaic cell in comparison with a nonferroelectric one.

Ferroelectricity-enhanced photovoltaic effects, although an emerging area of research, have been primarily observed only in traditional all-inorganic ferroelectric materials.[18,19] Obvious advantages[19−21] in using ferroelectric photovoltaic materials include the possibility of generating a large V_{OC}, facile separation of charge carriers, slow recombination, and long carrier diffusion lengths.

In the context of lead halide perovskites, it becomes natural to think of ferroelectricity for two obvious reasons. The organic units carry dipoles, which is the prerequisite of any ferroelectric material. In addition, many Pb^{2+}-containing inorganic materials are known to give rise to ferroelectricity arising from its lone pair,[22] which helps to distort it from a centrosymmetric position, thereby generating a dipole locally. Thus, the question whether lead halide perovskites are ferroelectric or not was asked early on, but surprisingly, this seemingly simple question has not been settled so far despite extensive investigations.[6,23−28] There are a large number of groups committed on either end of this debate, which persists even today. There are also suggestions that the material may be driven dynamically to a ferroelectric state under photoexcitation, while the ground state is not ferroelectric.[29]

The most direct way to determine whether a material is ferroelectric or not is to measure its induced polarization (P) as a function of an applied electric field (E). A typical ferroelectric state shows a hysteretic P−E loop, with remnant spontaneous polarization at zero applied field strength, as shown in Figure 2.

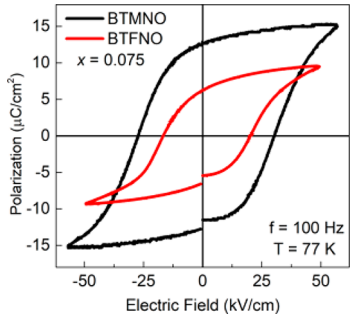

Figure 2. P−E loop in a typical ferroelectric material. Reproduced from ref 30. Copyright 2018 American Chemical Society.

There have been several P−E measurements reported in the literature with conflicting claims.[23,24,31,32] The uncertainty in such P−E loop measurements arise in this case from these perovskites being electrically very lossy; this often gives rise to spurious opening of P−E loops[33] complicating the interpretation. The other popular route to probe the possibility of ferroelectricity in any material is to measure its ability to generate a second harmonic or, in other words, light with twice the frequency of the incident light. Second harmonic generation (SHG) is a commonly used technique to determine whether the crystal structure of a material is polar, a primary requirement for any system to be ferroelectric. SHG is a nonlinear optical effect observed only in materials with finite second-order susceptibility. Thus, SHG is observed only in noncentrosymmetric or polar crystals and surfaces because

Received: June 14, 2018
Accepted: July 6, 2018
Published: July 17, 2018

DOI: 10.1021/acsenergylett.8b00999
ACS Energy Lett. 2018, 3, 1887−1891

symmetry requires that the second-order susceptibility be zero for centrosymmetric systems. This method has been extensively used in probing a variety of ferroelectric materials in the past. It turns out that distinctive properties of lead halide perovskites, compared to other traditional materials, demand certain precautions while being probed by this well-established technique.

A widely used method to check for the presence of the center of inversion in a material is to measure the SHG efficiency by the Kurtz–Perry method,[34] where the intensity of the second harmonic generated by a polycrystalline powder sample is compared with that generated by a SHG standard, like urea, potassium dihydrogen phosphate (KDP), etc. Highly intense laser sources are necessary to measure SHG because the intensity of this second-order effect is several orders of magnitude lower than the incident intensity. Almost all applications of SHG use pulsed laser sources at 800 or 1064 nm as these are the most commonly available high-power sources on the market. The second harmonic generated, if any, from these primary sources will be at 400 nm (3.1 eV) and 532 nm (2.3 eV) for 800 and 1064 nm pumps, respectively. Since the bandgap of conventional ferroelectric materials is rarely smaller[30] than 2.3 eV and often larger than 3.1 eV, probing wavelengths of 800 and 1064 nm provide convenient choices. For instance, bandgaps of $BaTiO_3$ and $PbTiO_3$, which are well-known polar (and ferroelectric) materials, are 3.2 and 3.8 eV, respectively. Unfortunately, these laser sources cannot be used for materials with bandgaps smaller than 2.3 eV. This is precisely the problem, not appreciated enough, with halide perovskites $CH_3NH_3PbI_3$ with a bandgap of 1.55 eV and $CH_3NH_3PbBr_3$ with a bandgap of 2.2 eV. In both compounds, the second harmonic at 400 nm (3.1 eV) or 532 nm (2.3 eV) from a fundamental excitation at 800 or 1064 nm, if at all generated, would be strongly absorbed by the material itself. Thus, a proper SHG measurement in these compounds including $CH_3NH_3PbI_3$ requires the use of wavelengths longer than 1720 nm, such that the second harmonic with a wavelength longer than 860 nm has a sub-bandgap energy (<1.55 eV) for the iodide. This prompted us to use a 1800 nm pulsed laser source to measure the SHG efficiency in these compounds, such that the second harmonic generated, if any, at 900 nm (see Figure 3) was still below the bandgap.[26,35] However, $CH(NH_2)_2PbI_3$, with a lower bandgap[36] of 1.41 eV, would require a fundamental excitation wavelength longer than 1800 nm (0.69 eV) so that the second harmonic, if any, does not lie within the absorption edge.

It is furthermore important to consider the hybrid organic–inorganic nature of the lead perovskites at the time of choice of the SHG pump wavelength. The organic components of these materials introduce vibrations as well as vibrational overtones in the infrared spectrum. Thus, not only is it important to ensure that SHG pump excitation energies are less than half of the bandgap but it is also essential to adjust the pump energy to avoid overlap with any strong sub-bandgap absorbances in the material. This is illustrated in Figure 3. It thus becomes particularly important to ensure sample transparency in these two wavelength regions in order to determine the SHG response from the bulk. This important aspect has received little attention so far in the community.

There is often the expectation that a single-crystal sample is better than polycrystalline ones. This is generally true, but it turns out that in the case of SHG measurements, performed on polycrystalline pellets, rather than on single crystals, in

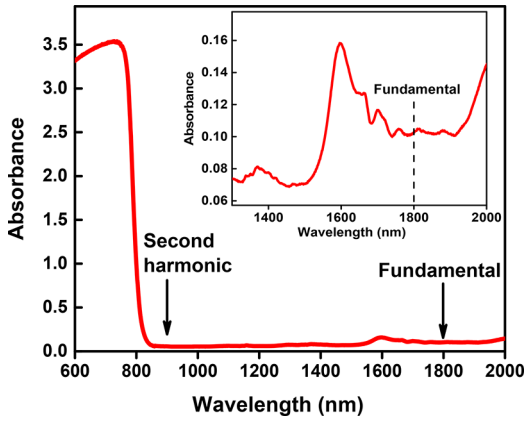

Figure 3. Choosing the fundamental excitation for SHG from the absorption spectrum of the material. This data has been taken on a $CH_3NH_3PbI_3$ sample. The inset shows an expanded view of the absorbance spectra in the near-IR region, where the absorbance features at around 1600 nm arise from overtones of the N–H stretch.[37]

principle avoids problems that may arise from phase mismatch and simplifies the interpretation of SHG responses. Further, if nonindex-matched, nontransmissive solids are used, the SHG signal that is generated (if any) emerges over a uniform co-sinusoidal lobe. In this case, the SHG signal has no strong directional dependence and can be collected in a wider range of angles. It is however still important to ensure that the crystallite sizes of the polycrystalline material be larger than the size of the wavelength of light to ensure a significant SHG response. Due to the necessity of using longer wavelengths to probe SHG in these perovskite compounds, the crystallite size becomes a relevant point to worry about in these cases. Measuring SHG response at different fundamental excitation wavelengths and particle sizes is a good way to check for true SHG from the bulk of the sample, as shown in a study[38] on germanium iodide perovskites.

Unlike most other materials, SHG measurements of perovskites are complicated by the existence of other nonlinearities. For example, these materials are now recognized[39,40] to possess anti-Stokes emission near the band edge. This phenomenon[39,40] allows these materials to absorb sub-bandgap light and subsequently emit at their usual emission band. The residual energy required for this up-conversion arises from thermal energy from the ambient. While this process scales linearly with power, lead halide perovskites are further known to exhibit substantial third-order nonlinear susceptibilities that scale nonlinearly with power. Due to the existence of these alternate nonlinear processes, it is necessary to completely isolate the SHG response spectrally to avoid contamination with other linear and nonlinear optical processes that occur in these materials. This is exemplified in Figure 4, which shows[41] the emission spectra under excitation at 1.03 eV (1204 nm).

Photoluminescence (PL) emission from the material is evident even under 1800 nm laser excitation of $CH_3NH_3PbI_3$ (see Figure 5).[26] Also, a broad emission in the relevant wavelength range in the case of $CH_3NH_3PbBr_3$ leaves ambiguity in the conclusion of the presence of SHG response (see Figure 2 of ref 27.). In most cases, quantification of the SHG signal thus makes it necessary to subtract out the background produced due to other nonlinearities. For example,

DOI: 10.1021/acsenergylett.8b00999
ACS Energy Lett. 2018, 3, 1887–1891

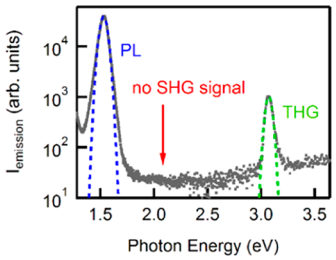

Figure 4. Emission spectra of $MAPbI_3$ under excitation at 1.03 eV. Reproduced from ref 41. Copyright 2015 American Chemical Society.

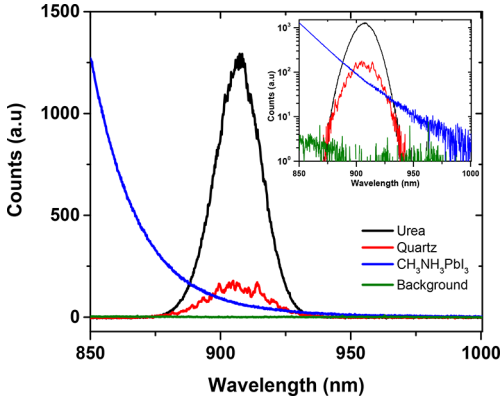

Figure 5. Spectra of the second harmonic generated at 900 nm, with a fundamental excitation of 1800 nm, measured on urea (in black), quartz (in red), and $CH_3NH_3PbI_3$ (in blue) along with the detector background shown in green. The inset shows the intensity plotted on the log scale. Reproduced from ref 26. Copyright 2016 American Chemical Society.

the monotonic PL background shown[26] in Figure 5 is incompatible with the SHG signal shape, which is expected to be essentially Gaussian (of a spectral width similar to the incident pulse), as also observed in urea and quartz, the SHG standards used. This requires that we record the region of interest around the expected second harmonic signal in a spectrally resolved manner and not monitor the intensity at exactly the point of doubled frequency with respect to the probing fundamental source frequency. From Figure 6, measuring the intensity at $2\nu_f$, double the fundamental frequency where the SHG signal is expected, would give the intensity value as *A*, while the true SHG intensity, *B*, is obtained after subtracting the background from the measured spectrum of the sample recorded in an extended frequency range. *A* is clearly larger than *B*, which would lead to a spurious value of the SHG intensity, if only a single-point intensity measurement would be performed. Note that Figure 6 is a simulation that combines actual $MAPbI_3$ background emission with the expected Gaussian profile from the second harmonic. The latter has never been observed in our experiments but hypothetically added in this figure to illustrate the point. Availability of the spectrum of SHG allows us to define precisely the intensity of the true SHG signal over and above the background signal that is often considerably intense in these materials.

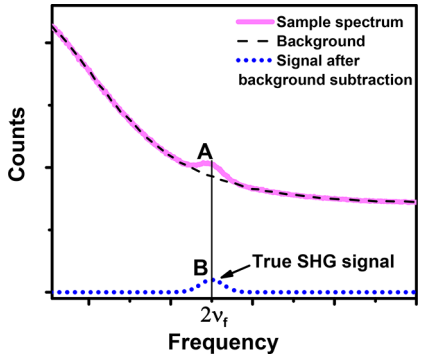

Figure 6. Schematic illustrating the necessity for spectrally resolved measurement of the SHG signal. The solid line shows the spectrum from the sample in the region of double the fundamental frequency $2\nu_f$, which contains both the SHG signal and background.

Although several studies of SHG in lead halide perovskites already exist, it is evident that significant progress is still expected to take place on several fronts. For example, while ensemble pump−probe studies suggest[35] the absence of a macroscopic ground state as well as light-induced ferroelectric polarization, results from SHG spatial microscopy studies[28] have been interpreted to suggest the existence of smaller domains. While some studies[42,43] have used the strong third harmonic response (THG) against the low SHG signal to conclude that the small SHG signal measured could be due to local symmetry breaking effects, some conclude that second harmonic generated could be due to large polar domains.[44] Studies that correlate spatiotemporal SHG responses with local microstructure will thus shine more light on the unusual properties of both the ground and excited states of perovskites and help understand these materials on both the macroscopic and microscopic scales.

Sharada Govinda
Bhushan P. Kore
Pratibha Mahale
Anshu Pandey
D. D. Sarma*
Solid State and Structural Chemistry Unit, Indian Institute of Science, Bengaluru 560012, India

AUTHOR INFORMATION

Corresponding Author
*E-mail: sarma@iisc.ac.in.
ORCID
Bhushan P. Kore: 0000-0003-3921-6194
Anshu Pandey: 0000-0003-3195-1522
D. D. Sarma: 0000-0001-6433-1069

Notes
Views expressed in this Viewpoint are those of the authors and not necessarily the views of the ACS.
The authors declare no competing financial interest.

ACKNOWLEDGMENTS

The authors thank the Department of Science and Technology for support. S.G. acknowledges CSIR for a student fellowship. B.P.K. acknowledges UGC, India for a D.S. Kothari Postdoctoral Fellowship. D.D.S. thanks Jemsetji Tata Trust for support.

DOI: 10.1021/acsenergylett.8b00999
ACS Energy Lett. 2018, 3, 1887−1891

REFERENCES

(1) Yoon, H.; Kang, S. M.; Lee, J.-K.; Choi, M. Hysteresis-Free Low-Temperature-Processed Planar Perovskite Solar Cells with 19.1% Efficiency. *Energy Environ. Sci.* **2016**, *9*, 2262−2266.

(2) Bi, D.; Tress, W.; Dar, M. I.; Gao, P.; Luo, J.; Renevier, C.; Schenk, K.; Abate, A.; Giordano, F.; Correa Baena, J.-P.; et al. Efficient Luminescent Solar Cells based on Tailored Mixed-Cation Perovskites. *Sci. Adv.* **2016**, *2*, e1501170.

(3) McMeekin, D. P.; Sadoughi, G.; Rehman, W.; Eperon, G. E.; Saliba, M.; Hörantner, M. T.; Haghighirad, A.; Sakai, N.; Korte, L.; Rech, B.; et al. A Mixed-Cation Lead Mixed-Halide Perovskite Absorber for Tandem Solar Cells. *Science* **2016**, *351*, 151−155.

(4) Saliba, M.; Matsui, T.; Seo, J.-Y.; Domanski, K.; Correa-Baena, J.-P.; Nazeeruddin, M. K.; Zakeeruddin, S. M.; Tress, W.; Abate, A.; Hagfeldt, A.; Gratzel, M. Cesium-Containing Triple Cation Perovskite Solar Cells: Improved Stability, Reproducibility and High Efficiency. *Energy Environ. Sci.* **2016**, *9*, 1989−1997.

(5) Kojima, A.; Teshima, K.; Shirai, Y.; Miyasaka, T. Organometal Halide Perovskites as Visible-Light Sensitizers for Photovoltaic Cells. *J. Am. Chem. Soc.* **2009**, *131*, 6050−6051.

(6) Baikie, T.; Fang, Y.; Kadro, J. M.; Schreyer, M.; Wei, F.; Mhaisalkar, S. G.; Graetzel, M.; White, T. J. Synthesis and Crystal Chemistry of the Hybrid Perovskite $(CH_3NH_3)PbI_3$ for Solid-State Sensitised Solar Cell Applications. *J. Mater. Chem. A* **2013**, *1*, 5628−5641.

(7) Xing, G.; Mathews, N.; Sun, S.; Lim, S. S.; Lam, Y. M.; Grätzel, M.; Mhaisalkar, S.; Sum, T. C. Long-Range Balanced Electron- and Hole-Transport Lengths in Organic-Inorganic $CH_3NH_3PbI_3$. *Science* **2013**, *342*, 344−347.

(8) Stranks, S. D.; Eperon, G. E.; Grancini, G.; Menelaou, C.; Alcocer, M. J. P.; Leijtens, T.; Herz, L. M.; Petrozza, A.; Snaith, H. J. Electron-Hole Diffusion Lengths Exceeding 1 Micrometer in an Organometal Trihalide Perovskite Absorber. *Science* **2013**, *342*, 341−344.

(9) Shirayama, M.; Kadowaki, H.; Miyadera, T.; Sugita, T.; Tamakoshi, M.; Kato, M.; Fujiseki, T.; Murata, D.; Hara, S.; Murakami, T. N.; et al. Optical Transitions in Hybrid Perovskite Solar Cells: Ellipsometry, Density Functional Theory, and Quantum Efficiency Analyses for $CH_3NH_3PbI_3$. *Phys. Rev. Appl.* **2016**, *5*, 014012.

(10) Wehrenfennig, C.; Eperon, G. E.; Johnston, M. B.; Snaith, H. J.; Herz, L. M. High Charge Carrier Mobilities and Lifetimes in Organolead Trihalide Perovskites. *Adv. Mater.* **2014**, *26*, 1584−1589.

(11) Bi, Y.; Hutter, E. M.; Fang, Y.; Dong, Q.; Huang, J.; Savenije, T. J. Charge Carrier Lifetimes Exceeding 15 μs in Methylammonium Lead Iodide Single Crystals. *J. Phys. Chem. Lett.* **2016**, *7*, 923−928.

(12) Dong, Q.; Fang, Y.; Shao, Y.; Mulligan, P.; Qiu, J.; Cao, L.; Huang, J. Electron-Hole Diffusion Lengths > 175 μm in Solution-Grown $CH_3NH_3PbI_3$ Single Crystals. *Science* **2015**, *347*, 967−970.

(13) Ishihara, T. Optical Properties of PbI-based Perovskite Structures. *J. Lumin.* **1994**, *60-61*, 269−274.

(14) Saba, M.; Cadelano, M.; Marongiu, D.; Chen, F.; Sarritzu, V.; Sestu, N.; Figus, C.; Aresti, M.; Piras, R.; Geddo Lehmann, A.; et al. Correlated Electron−Hole Plasma in Organometal Perovskites. *Nat. Commun.* **2014**, *5*, 5049.

(15) Galkowski, K.; Mitioglu, A.; Miyata, A.; Plochocka, P.; Portugall, O.; Eperon, G. E.; Wang, J. T.-W.; Stergiopoulos, T.; Stranks, S. D.; Snaith, H. J.; et al. Determination of the Exciton Binding Energy and Effective Masses for Methylammonium and Formamidinium Lead Tri-halide Perovskite Semiconductors. *Energy Environ. Sci.* **2016**, *9*, 962−970.

(16) Liu, M.; Johnston, M. B.; Snaith, H. J. Efficient Planar Heterojunction Perovskite Solar Cells by Vapour Deposition. *Nature* **2013**, *501*, 395−398.

(17) Brandt, R. E.; Stevanović, V.; Ginley, D. S.; Buonassisi, T. Identifying Defect-Tolerant Semiconductors with High Minority-Carrier Lifetimes: Beyond Hybrid Lead Halide Perovskites. *MRS Commun.* **2015**, *5*, 265−275.

(18) Yang, S. Y.; Seidel, J.; Byrnes, S. J.; Shafer, P.; Yang, C. H.; Rossell, M. D.; Yu, P.; Chu, Y. H.; Scott, J. F.; Ager, J. W.; et al. Above-Bandgap Voltages from Ferroelectric Photovoltaic Devices. *Nat. Nanotechnol.* **2010**, *5*, 143−147.

(19) Kreisel, J.; Alexe, M.; Thomas, P. A. A Photoferroelectric Material is More than the Sum of its Parts. *Nat. Mater.* **2012**, *11*, 260.

(20) Huang, H. Solar energy: Ferroelectric Photovoltaics. *Nat. Photonics* **2010**, *4*, 134−135.

(21) Frost, J. M.; Butler, K. T.; Brivio, F.; Hendon, C. H.; van Schilfgaarde, M.; Walsh, A. Atomistic Origins of High-Performance in Hybrid Halide Perovskite Solar Cells. *Nano Lett.* **2014**, *14*, 2584−2590.

(22) Walsh, A.; Payne, D. J.; Egdell, R. G.; Watson, G. W. Stereochemistry of Post-Transition Metal Oxides: Revision of the Classical Lone Pair Model. *Chem. Soc. Rev.* **2011**, *40*, 4455−4463.

(23) Stoumpos, C. C.; Malliakas, C. D.; Kanatzidis, M. G. Semiconducting Tin and Lead Iodide Perovskites with Organic Cations: Phase Transitions, High Mobilities, and Near-Infrared Photoluminescent Properties. *Inorg. Chem.* **2013**, *52*, 9019−9038.

(24) Fan, Z.; Xiao, J.; Sun, K.; Chen, L.; Hu, Y.; Ouyang, J.; Ong, K. P.; Zeng, K.; Wang, J. Ferroelectricity of $CH_3NH_3PbI_3$ Perovskite. *J. Phys. Chem. Lett.* **2015**, *6*, 1155−1161.

(25) Kim, H.-S.; Kim, S. K.; Kim, B. J.; Shin, K.-S.; Gupta, M. K.; Jung, H. S.; Kim, S.-W.; Park, N.-G. Ferroelectric Polarization in $CH_3NH_3PbI_3$ Perovskite. *J. Phys. Chem. Lett.* **2015**, *6*, 1729−1735.

(26) Sharada, G.; Mahale, P.; Kore, B. P.; Mukherjee, S.; Pavan, M. S.; De, C.; Ghara, S.; Sundaresan, A.; Pandey, A.; Guru Row, T. N.; et al. Is $CH_3NH_3PbI_3$ Polar? *J. Phys. Chem. Lett.* **2016**, *7*, 2412−2419.

(27) Rakita, Y.; Meirzadeh, E.; Bendikov, T.; Kalchenko, V.; Lubomirsky, I.; Hodes, G.; Ehre, D.; Cahen, D. $CH_3NH_3PbBr_3$ is not Pyroelectric, Excluding Ferroelectric-Enhanced Photovoltaic Performance. *APL Mater.* **2016**, *4*, 051101.

(28) Rakita, Y.; Bar-Elli, O.; Meirzadeh, E.; Kaslasi, H.; Peleg, Y.; Hodes, G.; Lubomirsky, I.; Oron, D.; Ehre, D.; Cahen, D. Tetragonal $CH_3NH_3PbI_3$ is Ferroelectric. *Proc. Natl. Acad. Sci. U. S. A.* **2017**, *114*, E5504−E5512.

(29) Wang, P.; Zhao, J.; Wei, L.; Zhu, Q.; Xie, S.; Liu, J.; Meng, X.; Li, J. Photo-Induced Ferroelectric Switching in Perovskite $CH_3NH_3PbI_3$ Films. *Nanoscale* **2017**, *9*, 3806−3817.

(30) Das, S.; Ghara, S.; Mahadevan, P.; Sundaresan, A.; Gopalakrishnan, J.; Sarma, D. D. Designing a Lower Band Gap Bulk Ferroelectric Material with a Sizable Polarization at Room Temperature. *ACS Energy Lett.* **2018**, *3*, 1176−1182.

(31) Beilsten-Edmands, J.; Eperon, G. E.; Johnson, R. D.; Snaith, H. J.; Radaelli, P. G. Non-ferroelectric Nature of the Conductance Hysteresis in $CH_3NH_3PbI_3$ Perovskite-based Photovoltaic Devices. *Appl. Phys. Lett.* **2015**, *106*, 173502.

(32) Xiao, Z.; Yuan, Y.; Shao, Y.; Wang, Q.; Dong, Q.; Bi, C.; Sharma, P.; Gruverman, A.; Huang, J. Giant Switchable Photovoltaic Effect in Organometal Trihalide Perovskite Devices. *Nat. Mater.* **2015**, *14*, 193−198.

(33) Scott, J. F. Ferroelectrics go Bananas. *J. Phys.: Condens. Matter* **2008**, *20*, 021001.

(34) Kurtz, S. K.; Perry, T. T. A Powder Technique for the Evaluation of Nonlinear Optical Materials. *J. Appl. Phys.* **1968**, *39*, 3798−3813.

(35) Govinda, S.; Kore, B. P.; Bokdam, M.; Mahale, P.; Kumar, A.; Pal, S.; Bhattacharyya, B.; Lahnsteiner, J.; Kresse, G.; Franchini, C.; et al. Behavior of Methylammonium Dipoles in $MAPbX_3$ (X = Br and I). *J. Phys. Chem. Lett.* **2017**, *8*, 4113−4121.

(36) Zhumekenov, A. A.; Saidaminov, M. I.; Haque, M. A.; Alarousu, E.; Sarmah, S. P.; Murali, B.; Dursun, I.; Miao, X.-H.; Abdelhady, A. L.; Wu, T.; et al. Formamidinium Lead Halide Perovskite Crystals with Unprecedented Long Carrier Dynamics and Diffusion Length. *ACS Energy Lett.* **2016**, *1*, 32−37.

(37) Pérez-Osorio, M. A.; Milot, R. L.; Filip, M. R.; Patel, J. B.; Herz, L. M.; Johnston, M. B.; Giustino, F. Vibrational Properties of the Organic−Inorganic Halide Perovskite $CH_3NH_3PbI_3$ from Theory and Experiment: Factor Group Analysis, First-Principles Calculations, and

DOI: 10.1021/acsenergylett.8b00999
ACS Energy Lett. 2018, 3, 1887−1891

Low-Temperature Infrared Spectra. *J. Phys. Chem. C* **2015**, *119*, 25703−25718.
(38) Stoumpos, C. C.; Frazer, L.; Clark, D. J.; Kim, Y. S.; Rhim, S. H.; Freeman, A. J.; Ketterson, J. B.; Jang, J. I.; Kanatzidis, M. G. Hybrid Germanium Iodide Perovskite Semiconductors: Active Lone Pairs, Structural Distortions, Direct and Indirect Energy Gaps, and Strong Nonlinear Optical Properties. *J. Am. Chem. Soc.* **2015**, *137*, 6804−6819.
(39) Ha, S.-T.; Shen, C.; Zhang, J.; Xiong, Q. Laser Cooling of Organic−Inorganic Lead Halide Perovskites. *Nat. Photonics* **2016**, *10*, 115−121.
(40) Morozov, Y. V.; Zhang, S.; Brennan, M. C.; Janko, B.; Kuno, M. Photoluminescence Up-Conversion in $CsPbBr_3$ Nanocrystals. *ACS Energy Lett.* **2017**, *2*, 2514−2515.
(41) Yamada, Y.; Yamada, T.; Phuong, L. Q.; Maruyama, N.; Nishimura, H.; Wakamiya, A.; Murata, Y.; Kanemitsu, Y. Dynamic Optical Properties of $CH_3NH_3PbI_3$ Single Crystals As Revealed by One- and Two-Photon Excited Photoluminescence Measurements. *J. Am. Chem. Soc.* **2015**, *137*, 10456−10459.
(42) Clark, D. J.; Stoumpos, C. C.; Saouma, F. O.; Kanatzidis, M. G.; Jang, J. I. Polarization-Selective Three-Photon Absorption and Subsequent Photoluminescence in $CsPbBr_3$ Single Crystal at Room Temperature. *Phys. Rev. B: Condens. Matter Mater. Phys.* **2016**, *93*, 195202.
(43) Abdelwahab, I.; Grinblat, G.; Leng, K.; Li, Y.; Chi, X.; Rusydi, A.; Maier, S. A.; Loh, K. P. Highly Enhanced Third-Harmonic Generation in 2D Perovskites at Excitonic Resonances. *ACS Nano* **2018**, *12*, 644−650.
(44) Stoumpos, C. C.; Cao, D. H.; Clark, D. J.; Young, J.; Rondinelli, J. M.; Jang, J. I.; Hupp, J. T.; Kanatzidis, M. G. Ruddlesden−Popper Hybrid Lead Iodide Perovskite 2D Homologous Semiconductors. *Chem. Mater.* **2016**, *28*, 2852−2867.

DOI: 10.1021/acsenergylett.8b00999
ACS Energy Lett. 2018, 3, 1887−1891